

The limit shape of large alternating sign matrices

F. Colomo and A.G. Pronko

ABSTRACT. The problem of the limit shape of large alternating sign matrices (ASMs) is addressed by studying the emptiness formation probability (EFP) in the domain-wall six-vertex model. Assuming that the limit shape arises in correspondence to the ‘condensation’ of almost all solutions of the saddle-point equations for certain multiple integral representation for EFP, a conjectural expression for the limit shape of large ASMs is derived. The case of 3-enumerated ASMs is also considered.

1. Introduction

An alternating sign matrix (ASM) is a matrix of 1’s, 0’s and -1 ’s such that in each row and column, all nonzero entries alternate in sign, and the first and the last nonzero entries are 1’s. In a weighted enumeration, or q -enumeration, ASMs are counted with a weight q^k , where k is the total number of -1 ’s in each matrix. There are many nice results concerning ASMs, mainly devoted to their various enumerations; for a review see, e.g., book [1].

In this paper, we address the problem of the limit shape of large ASMs. The problem comes out from the fact that in ASMs their corner regions mostly contain 0’s while in the interior there are many nonzero entries. As the size of ASMs increases, the probabilities of finding 1’s and -1 ’s in their entries in the corner regions vanish, while in the central region these probabilities remain finite. When considering very large ASMs in an appropriate scaling limit, (e.g., when large matrices are scaled to a unit square), one can expect that such regions become sharply separated. Assuming that the very fact of this phase separation is somehow ascertained, an interesting question which can be then addressed concerns finding an explicit equation for the spatial curve separating these two regions [2].

In essence, this curve can be regarded as an Arctic curve for ASMs, similar to the Arctic Circle of domino tilings of large Aztec diamonds [3]. Since the Arctic curve determines the shape of the internal, or ‘temperate’, region of ASMs, one can refer to this curve as the limit shape of large ASMs (cf. [4]). More generally, one can address the same problem for the case of q -enumerated ASMs. Then the case $q = 2$ corresponds to the Arctic Circle of the domino tilings (see equation (10) below). The main result of the present paper consists in providing explicit expressions, albeit conjectural, for the limit shapes of 1- and 3-enumerated ASMs. They are given by equations (13) and (16), respectively.

To treat the problem, we exploit the one-to-one correspondence between ASMs and configurations of the six-vertex model, which has been found and efficiently

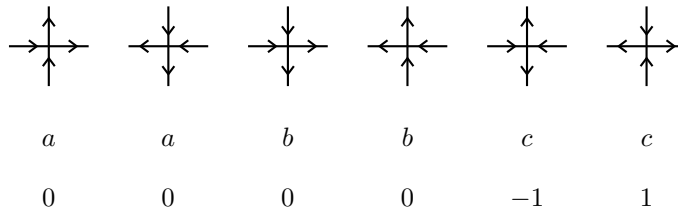


FIGURE 1. The six allowed arrow configurations, their weights, and the corresponding entries of ASMs.

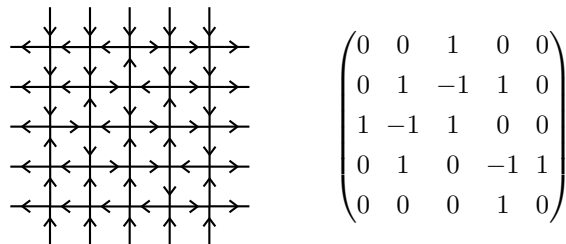


FIGURE 2. A possible configuration of the six-vertex model with DWBC and the corresponding ASM, for $N = 5$.

used in papers [5–7]. This correspondence takes place when the six-vertex model is considered with the so-called domain wall boundary conditions (DWBC). The six-vertex model with these boundary conditions has been originally introduced and studied in [8–10].

Using the standard description of local states in terms of arrows (see, e.g., [11]), DWBC mean that the model is considered on a square lattice of N vertical and N horizontal lines, where the arrows on all external horizontal edges point outward, while the arrows on all external vertical edges point inward. Then, the 0's in ASM's entries correspond to the vertices of weights a and b , while both 1's and -1 's correspond to vertices of weight c , as shown in Figure 1. Figure 2 shows a possible configuration of the six-vertex model DWBC and the corresponding ASM.

To count ASMs, the weights a , b , c are to be put all to the same value, e.g., $a = b = c = 1$. In q -enumeration, ASMs are counted by taking $a = b = 1$ and $c = \sqrt{q}$, since in each configuration the vertices of type five and six come in pairs, in addition to N vertices of type six being always present due to DWBC.

The main tool which we use to address the problem of the Arctic curve of the domain-wall six-vertex model is a particular, non-local, correlation function, the so-called emptiness formation probability (EFP). In paper [12] a multiple integral representation for EFP has been derived. Here, we study the multiple integral representation for large size of the lattice (corresponding to large size of ASMs).

In our approach an important role is played by the conjecture that the Arctic curve appears in correspondence to the situation where almost all roots of the saddle-point equations condense to the same, known, value. In paper [13] this correspondence has been shown to hold in the free-fermion case (i.e., when the weights obey $a^2 + b^2 = c^2$), where the assumption of condensation allows one to recover the Arctic Circle (the limit shape of 2-enumerated ASMs). Outside the free-fermion case the correspondence between the Arctic curve and the condensation of

roots is only conjectural (hence we use below the term ‘condensation hypothesis’) and it seems it could hardly be proven, at least by the methods at our disposal.

The condensation hypothesis is based essentially on the following argument. EFP is, by construction, able to discriminate the spatial transition from a frozen to a temperate region in the scaling limit (jumping from one to zero exactly at the Arctic curve, i.e., at the curve where the spatial phase transition from order to disorder takes place). Thus, if the Arctic curve exists, the multiple integral representation for EFP must exhibit the above mentioned stepwise behaviour. In the free-fermion case, this stepwise behaviour is explained by the mechanism of condensation of roots of the saddle-point equations, which in turn can be reconducted to certain specific properties of the multiple integral representation for EFP. These properties appear to hold independently of the values of weights, thus supporting the validity of the condensation hypothesis beyond the free-fermion case. This allows us to formulate a recipe for deriving an equation for the Arctic curve. The total procedure is fulfilled here for the two cases of weights corresponding to 1- and 3-enumeration of ASMs.

In particular, the resulting equation for the Arctic curve describing the limit shape of large ASMs is in good agreement with the most refined numerical simulations available [14]. This could be regarded as confirming the condensation hypothesis together with the method used here for deriving of the Arctic curve.

Our paper is organized as follows. In the next Section we recall results of [12] on multiple integral representations. In Section 3 the condensation hypothesis is discussed, and a procedure for the derivation of limit shapes is explained. In Section 4 we derive the limit shape of 1- and 3-enumerated ASMs.

2. Emptiness formation probability

As in [12, 13], we call emptiness formation probability (EFP) and denote by $F_N^{(r,s)}$, where $r, s = 1, \dots, N$, the probability of having all arrows on the first s horizontal edges from the top of the lattice, located between r -th and $(r + 1)$ -th vertical lines (counted from the right), to be all pointing left.

With this definition, EFP measures the probability that all vertices in the top-left $(N - r) \times s$ sublattice have the same configuration of arrows, namely, with all arrows pointing left or downwards, or, equivalently, that these vertices are of type two (see Figure 1). This follows from the peculiarity of both DWBC and the six-vertex model rule of two incoming and two outgoing arrows at each lattice vertex (known also as the ‘ice-rule’). It is worth noticing that in principle one could define analogous correlation functions for the other three corners of the lattice. They would measure the probability that all vertices in a bottom-right (or top-right, or bottom-left) rectangular sublattice of given size are of type one (or three, or four, respectively). It is clear that all these correlation functions can be obtained from the EFP defined above on the basis of symmetry considerations.

In the language of ASMs the definition of EFP implies that it measures the probability that all entries in the top-left $(N - r) \times s$ block are 0’s. Clearly, fixing the size of ASMs, N , one can expect that EFP takes values closer to 1 as r and s approach the top left corner of the matrix, and takes values closer to 0 otherwise, e.g., while r and s approach its central region. More precisely, from the definition of EFP one expects that it is a non-increasing function of the variables $N - r$ and s for arbitrary fixed value of N .

To address the problem of spatial phase separation in the domain-wall six-vertex model and, therefore, the problem of the limit shape of ASMs, one has to consider the so-called scaling limit, i.e., the limit of large N, r, s with the ratios r/N and s/N kept fixed. Using standard arguments of statistical mechanics, one can argue that, if spatial phase separation occurs, then in the scaling limit EFP must be equal to 1 in the frozen region in the top-left corner of the lattice and to 0 in the disordered region in the centre. In other words, if spatial separation occurs, in the scaling limit EFP is expected to exhibit stepwise behaviour, with the jump occurring exactly at (the top-left ‘portion’ of) the Arctic curve.

In [12] several equivalent representations for EFP were given. For what follows we shall need two representations in terms of multiple integrals. To recall these formulae, we introduce some objects first.

An important role in our considerations is played by the function $h_N(z) = h_N(z; \Delta, t)$, where Δ and t are to be regarded as parameters,

$$\Delta := \frac{a^2 + b^2 - c^2}{2ab}, \quad t := \frac{b}{a},$$

while z is to be treated as a variable. This function, defined as a generating function, is a polynomial of degree $(N - 1)$ in z ,

$$h_N(z) := \sum_{r=1}^N H_N^{(r)} z^{r-1}, \quad h_N(1) = 1.$$

Here the quantity $H_N^{(r)} = H_N^{(r)}(\Delta, t)$ is a boundary correlation function, introduced in [15]. Namely, it is the probability that the sole vertex of type six (having weight c), residing in the first row, appears at r -th position from the right. At $t = 1$ the function $h_N(z)$ has a special meaning as the generating function for refined q -enumerations of ASMs, with q and Δ related by $\Delta = 1 - q/2$. Our derivation of the limit shapes below involves essentially the known explicit expressions for this generating function at some particular values of q .

For $s = 1, \dots, N$, we define functions

$$h_{N,s}(z_1, \dots, z_s) = \prod_{1 \leq j < k \leq s} (z_j - z_k)^{-1} \det_{1 \leq j, k \leq s} [z_j^{k-1} (z_j - 1)^{s-k} h_{N-k+1}(z_j)]. \quad (1)$$

These functions can be regarded as multi-variable generalizations of $h_N(z)$, in the sense that $h_{N,1}(z) = h_N(z)$. It can be easily checked that

$$h_{N,s+1}(z_1, \dots, z_s, 1) = h_{N,s}(z_1, \dots, z_s). \quad (2)$$

One also has

$$h_{N,s+1}(z_1, \dots, z_s, 0) = h_N(0) h_{N-1,s}(z_1, \dots, z_s). \quad (3)$$

Properties (2) and (3) are used in what follows.

We are now ready to turn to the multiple integral representations. In [12], the following multiple integral representation has been obtained

$$\begin{aligned} F_N^{(r,s)} &= \frac{(-1)^s}{(2\pi i)^s} \oint_{C_0} \dots \oint_{C_0} \prod_{j=1}^s \frac{[(t^2 - 2t\Delta)z_j + 1]^{s-j}}{z_j^r (z_j - 1)^{s-j+1}} \\ &\quad \times \prod_{1 \leq j < k \leq s} \frac{z_j - z_k}{t^2 z_j z_k - 2t\Delta z_j + 1} h_{N,s}(z_1, \dots, z_s) dz_1 \dots dz_s. \quad (4) \end{aligned}$$

Here C_0 denotes some simple anticlockwise oriented contour surrounding the point $z = 0$ and no other singularity of the integrand. Formula (4) has been derived in [12], using the quantum inverse scattering method [16, 17] and the results of papers [9, 10, 15]. This formula has also been discussed in [13] (see equation (3.6) therein).

In [12], the following equivalent representation has been also given:

$$F_N^{(r,s)} = \frac{(-1)^{s(s+1)/2} Z_s}{s!(2\pi i)^s a^{s(s-1)} c^s} \oint_{C_0} \cdots \oint_{C_0} \prod_{j=1}^s \frac{[(t^2 - 2t\Delta)z_j + 1]^{s-1}}{z_j^r (z_j - 1)^s} \\ \times \prod_{\substack{j,k=1 \\ j \neq k}}^s \frac{1}{t^2 z_j z_k - 2t\Delta z_j + 1} \prod_{1 \leq j < k \leq s} (z_k - z_j)^2 \\ \times h_{N,s}(z_1, \dots, z_s) h_{s,s}(u_1, \dots, u_s) dz_1 \cdots dz_s. \quad (5)$$

Here Z_s denotes the partition function of the six-vertex model with DWBC on an $s \times s$ lattice, and

$$u_j := -\frac{z_j - 1}{(t^2 - 2t\Delta)z_j + 1}. \quad (6)$$

For later use we emphasize that the integrand of (5) is just the symmetrized version of the integrand of (4), with respect to permutations of the integration variables z_1, \dots, z_s . This follows through the symmetrization procedure explained in [18], and some additional identity proven in [12].

We are interested in the behaviour of EFP in the so-called scaling limit, that is in the limit where r , s and N are all large, with the ratios r/N and s/N kept finite (and smaller than 1). Applying standard arguments of saddle-point analysis to representation (5), namely by writing its integrand in exponential form, and by setting the partial derivatives of the exponent equal to zero, we obtain the following system of coupled saddle-point equations

$$-\frac{s}{z_j - 1} + \frac{s(t^2 - 2t\Delta)}{(t^2 - 2t\Delta)z_j + 1} - \frac{r}{z_j} + \sum_{\substack{k=1 \\ k \neq j}}^s \frac{2}{z_j - z_k} \\ + \sum_{\substack{k=1 \\ k \neq j}}^s \left(\frac{2\Delta t - t^2 z_k}{t^2 z_j z_k - 2\Delta t z_j + 1} - \frac{t^2 z_k}{t^2 z_j z_k - 2\Delta t z_k + 1} \right) + \frac{\partial}{\partial z_j} \log h_{N,s}(z_1, \dots, z_s) \\ - \frac{t^2 - 2\Delta t + 1}{[(t^2 - 2\Delta t)z_j + 1]^2} \frac{\partial}{\partial u_j} \log h_{s,s}(u_1, \dots, u_s) = 0. \quad (7)$$

In deriving these equations we have used the fact that quantities like $\log h_{N,s}$ are of order s^2 , and that their derivatives with respect to z_j 's are of order s ; all sub-leading contributions (estimated as $o(s)$) are neglected.

To evaluate the asymptotic behaviour of EFP in the scaling limit, which would allow one to address the problems of existence of spatial phase separation and find the corresponding Arctic curve, one needs, in principle, to be able to describe the solutions of saddle-point equations (7). Apparently, this task is a formidable one, at least because the last two terms in equations (7) are rather implicit. Even in the technically simpler case of $\Delta = 0$ (the free-fermion point) when these two terms can be found explicitly, the task remains rather complicated since in this case the saddle-point equations correspond to a matrix model with a triple logarithmic

singularity, or a ‘triple’ Penner model, and finding their solutions in general settings represents an open problem (see, for further details, discussion in [13]).

Nevertheless, it turns out that some interesting information can be extracted from saddle-point equations (7) provided we assume that some facts hold true a priori. Namely, we shall assume that EFP in the scaling limit develops a stepwise behaviour, with the jump from one to zero occurring at (the top-left portion of) the Arctic curve. In other words, we assume that the phase separation, and hence the Arctic curve, exists.

The existence of phase separation can be argued from statistical mechanics, by studying, for example, the influence of boundary conditions on the free energy per site [19]. Phase separation is also supported by previous studies on the six-vertex model from which we know that usually the phenomena are qualitatively similar for the whole range of values of the weights corresponding to the same regime (in the phase diagram) of the model [11]. On the other hand, from domino tilings studies it is known that the phase separation occurs in free-fermion case, $\Delta = 0$. Hence we can expect that this is a general fact for the whole disordered regime, $|\Delta| < 1$; the validity of this statement is supported by numerics [20, 21].

Assuming a priori the existence of the limit shape, or equivalently, the stepwise behaviour of EFP in the scaling limit, we shall argue that the location of the step correspond to a very particular, and relatively simple solution of the saddle-point equations (7). This, in turn, will give us a recipe for obtaining the equation of the Arctic curve, and hence the limit shape of ASMs.

3. Condensation hypothesis and ‘reduced saddle-point equation’

As already discussed, by assuming the existence of the phase separation, we require that EFP in the scaling limit, $N, r, s \rightarrow \infty$ with r/N and s/N kept fixed, has a stepwise behaviour, with the jump at the Arctic curve. Hence to address the problem of finding this curve one can try to explain how the multiple integral for EFP may have such a behaviour in the limit.

Intuitively speaking, it is clear that the value of EFP in the ordered region, where it must be equal to 1, can be explained by the fact that in this case the roots of equations (7) are such that integral (5) is governed by residues from certain poles rather than by contributions from the corresponding saddle-point contours. Below we show that these are the poles (for each integration variable) at point $z = 1$, and prove that indeed the cumulative residue at these poles over all variables is exactly 1. On the other hand, the value of EFP in the disordered region, where it must be equal to 0, can be explained simply by the fact that in this case no pole contributes to the integral (5), which is thus given by integration over the saddle-point contours, vanishing in the scaling limit.

According to the above picture the transition from one region to another, i.e., when EFP jumps from 1 to 0, can be associated to the situation where almost all the roots of saddle-point equations are located at the point $z = 1$, i.e., in correspondence to the pole relevant for the stepwise behaviour of EFP. Here ‘almost all’ means all but a vanishing fraction of roots. This is a very special solution of saddle-point equations, characterized by what can be called ‘total condensation’ of roots, which is defined more precisely below. It turns out that the condition of total condensation can be implemented efficiently, leading to the expression for a

curve in the unit square of the scaling limit variables, which, in view of the above considerations, we recognize as the Arctic curve.

In particular, the validity of the assumption of total condensation can be verified in the free-fermion case, $\Delta = 0$. In [13], it has been shown that indeed in this case the limit shape corresponds to the situation where almost all roots of equations (7), as $s \rightarrow \infty$, condense at the point $z = 1$. More precisely, it has been shown that assuming total condensation one can recover the Arctic curve, which in this case is the Arctic Circle (or ellipse), already known from previous studies [3]. On the other hand, as it can be easily seen from the equations in [13], restricting to the Arctic circle, one obtains for the resolvent of the saddle-point solutions a trivial expression, having just a single pole at $z = 1$, which implies precisely total condensation (see also discussion below). Thus, at $\Delta = 0$ one can verify the full correspondence between total condensation and the Arctic curve.

The possibility of total condensation for random matrix integrals in general, and for multiple integral (5) when specialized to the case of $\Delta = 0$ in particular, can be related to a simple fundamental property, namely, to the presence in the integrand of a pole at the same point in all s integration variables, z_1, \dots, z_s , which moreover must be exactly of order s (see discussion in [22,23]). On the other hand, in the case of $\Delta = 0$, the unit jump in the stepwise behaviour of the multiple is due to the fact that the cumulative residue over all variables z_1, \dots, z_s at this pole is equal to 1, i.e., to the value of the jump.

It is a remarkable fact that for the multiple integral representation for EFP these two crucial properties hold for generic values of Δ . The first property can be easily verified by direct inspection of formula (5). Verification of the second property could represent a difficult problem, but fortunately it can easily be solved provided that multiple integral representation (4) rather than (5) is used for the analysis. Indeed, basing on multiple integral representation (4), let us consider, for $r, s = 1, \dots, N$, the integral

$$I_N^{(r,s)} := \frac{(-1)^s}{(2\pi i)^s} \oint_{C_1^-} \cdots \oint_{C_1^-} \prod_{j=1}^s \frac{[(t^2 - 2t\Delta)z_j + 1]^{s-j}}{z_j^r (z_j - 1)^{s-j+1}} \\ \times \prod_{1 \leq j < k \leq s} \frac{z_j - z_k}{t^2 z_j z_k - 2t\Delta z_j + 1} h_{N,s}(z_1, \dots, z_s) dz_1 \cdots dz_s.$$

Here C_1^- is a closed contour in the complex plane enclosing point $z = 1$ and no other singularity of the integrand; the minus in the notation indicates negative (clockwise) orientation. We have

$$I_N^{(r,s)} = 1. \quad (8)$$

Indeed, performing integration in the variable z_s , and taking into account (2), identity (8) follows immediately by induction. Note that relation (8) implies the same relation for the integral with the integrand of (5), which is just the symmetrized version of the integrand of (4).

The fact that these two crucial properties still hold for generic values of Δ , together with the assumed stepwise behaviour of EFP in the scaling limit lead us to conjecture that the correspondence of limit shape and condensation of (almost) all roots of saddle-point equations (7) holds for generic values of Δ . Since we are not able to prove this statement, we call it here ‘condensation hypothesis’.

To treat the consequences of condensation of roots, we rely on results of papers [22, 23], where an analytic description of the mechanism of condensation has been provided, in the context of random matrix models with generic polynomial potentials with an additional logarithmic term (Penner models, [24]). Since these results do not depend on the explicit form of the potential but only on some of its properties it is reasonable to assume they still hold in more general situations, such as the one of multiple integral representation (5), where these properties are again observed, as discussed above.

To consider the scaling limit, $N, r, s \rightarrow \infty$, we define variables x and y such that

$$x := \frac{N-r}{N}, \quad y := \frac{s}{N}, \quad x, y \in [0, 1].$$

where, in general, $x, y \in [0, 1]$. Specifically, the top-left portion of limit shape for ASM's will be given as an equation for x and y , with these variables varying in the interval $[0, 1/2]$.

By ‘total condensation’ we mean that, as $s \rightarrow \infty$, almost all roots z_j of (7) have the value $z = 1$, in the sense that the amount of non-condensed roots is $o(s)$. This implies that at $s = \infty$ the density of roots is just the Dirac delta-function $\delta(z-1)$, or that the resolvent of the solution (the Green function) is $G(z) = (z-1)^{-1}$. Let s_c and s_n denote the numbers of condensed and non-condensed roots, $s_c + s_n = s$. Total condensation thus means that $s_c/s \rightarrow 1$ and $s_n/s \rightarrow 0$, as $s \rightarrow \infty$.

For an analytical treatment of the implication of the condensation of roots in the context of equations (7), we introduce here the concept of the ‘reduced saddle-point equation’. To this purpose we note that the non-condensed roots are only a vanishing fraction of the total number of roots, and thus that their contribution into sums over all roots can be neglected as s tends to infinity. Hence, assuming, without loss of generality, that z_j , where $j = 1, \dots, s_n$, is one of the non-condensed roots, we may pick up the j -th equation in (7) and simply set $z_k = 1$ for $k = s_n + 1, \dots, s$. For example, the first sum in (7) (the fourth term in the first line) then reduces to $2s/(z_j - 1)$, at leading order for large s , thus combining with the first term in (7). Similarly, one can easily evaluate the second sum, with a result partially combining with the second term in (7).

To evaluate contributions from the last two terms in (7) we use relations (2) and (3). For instance, due to property (2) function $h_{N,s}(z_1, \dots, z_s)$ simplifies to function $h_{N,s_n}(z_1, \dots, z_{s_n})$, which, in turn, for $N, s \rightarrow \infty$, and $s_n/N \sim 0$, can be evaluated for large s directly from its definition (1). In this way we obtain

$$\begin{aligned} \log h_{N,s}(z_1, \dots, z_s) \Big|_{z_{s_n+1}=\dots=z_s=1} &= \log h_{N,s_n}(z_1, \dots, z_{s_n}) \\ &= \sum_{k=1}^{s_n} \log h_N(z_k) + o(s). \end{aligned}$$

Here each term under the sum is of order N and hence estimated as of order s . The fact that $\log h_N(z)$ is of order N can be justified using statistical mechanics arguments; moreover this fact is transparent for the examples considered below.

Similarly, noticing that $u_k \rightarrow 0$ as $z_j \rightarrow 1$, see (6), and using property (3), we find that function $h_{s,s}(u_1, \dots, u_s)$ simplifies, modulo an unessential factor, to function $h_{s_n,s_n}(u_1, \dots, u_{s_n})$. Recalling that $h_{s_n,s_n}(u_1, \dots, u_{s_n})$ is a polynomial of order s_n in each of its variables, we obtain that its logarithm for large s is estimated

as $o(s)$. Thus we have

$$\begin{aligned} \log h_{s,s}(u_1, \dots, u_s) \Big|_{z_{s_n+1}=\dots=z_s=1} &= \sum_{k=s_n+1}^s \log h_k(0) + \log h_{s_n, s_n}(u_1, \dots, u_{s_n}) \\ &= C_1 s^2 + C_2 s + o(s). \end{aligned}$$

Here C_1 and C_2 are some quantities which do not depend on u_j ($j = 1, \dots, s_n$). After differentiating we find that the last term in (7) is estimated as $o(s)$, and can thus be neglected at the considered order.

As a result, writing simply z for z_j , we arrive at the following equation

$$\frac{y}{z-1} - \frac{1-x}{z} - \frac{t^2 y}{t^2 z - 2t\Delta + 1} + \lim_{N \rightarrow \infty} \frac{1}{N} \frac{\partial}{\partial z} \log h_N(z) = 0. \quad (9)$$

We call equation (9) the reduced saddle-point equation. The solutions of this equation give the non-condensed roots of (7) at total condensation.

As observed in [23], a necessary condition for the total condensation of roots of saddle-point equations like (7), is the presence of two coinciding non-condensed roots. In general this pair of coinciding real roots constitutes the germ of the cut which the resolvent develops when parameters are varied with respect to the situation of total condensation.

In our case, in view of the scenario depicted above, when the parameters x, y are varied away from the limit shape, towards the region where EFP assumes the value 1, such cut necessarily lies on the real axis, with $z > 1$. This implies that at condensation, in correspondence of the limit shape, these coinciding roots must lie on the real axis, in the interval $[1, \infty)$. Their position depends on the position of point (x, y) on the limit shape. Thus the value of these roots naturally parameterizes the limit shape between two contact points.

Summarizing, the condensation hypothesis leads to the following recipe for the derivation of limit shapes: we require (9) to have two coinciding roots, which moreover must run over the interval $[1, \infty)$. Denoting the value of these two roots by ω , we shall see below that as ω runs over the real axis from point $z = 1$ to point $z = \infty$, it parameterizes the top-left portion of the limit shape, from the contact point on the top (corresponding to $\omega = 1$) to the contact point on the left (corresponding to $\omega = \infty$).

An ingredient which is necessary for this programme, is the knowledge of the last term in (9). Fortunately, function $h_N(z)$ is explicitly known in some interesting cases. These are, for $t = 1$, the case of $\Delta = 1/2$, corresponding to usual enumeration of ASMs, and the case of $\Delta = -1/2$, corresponding to 3-enumerated ASMs; for generic t the function $h_N(z)$ is also known for $\Delta = 0$, corresponding to the six-vertex model in the free-fermion case (specializing further $t = 1$, one gets 2-enumerated ASMs).

To illustrate how the recipe is working, let us consider the case of $\Delta = 0$. We set also $t = 1$ for simplicity, so that function $h_N(z) = h_N(z; \Delta, t)$ in this case is just $h_N(z; 0, 1) = [(z+1)/2]^{N-1}$ (see, e.g., [13]). The reduced saddle-point equation reads

$$\frac{y}{z-1} - \frac{1-x}{z} + \frac{1-y}{z+1} = 0.$$

Denoting by $g(z)$ the function in the left-hand side, we require $g(z) = (z-\omega)^2 \tilde{g}(z)$ where $\tilde{g}(z)$ is regular near point $z = \omega$. This can be implemented by the system

of two equations $g(\omega) = 0$ and $g'(\omega) = 0$, where the prime denotes derivative, for unknowns x and y . Solving this system, we obtain

$$x = \frac{1}{\omega^2 + 1}, \quad y = \frac{(\omega - 1)^2}{2(\omega^2 + 1)}, \quad \omega \in [1, \infty).$$

Eliminating ω , we also have the equation for the limit shape

$$4x(1 - x) + 4y(1 - y) = 1. \quad (10)$$

Here x and y take values in interval $[0, 1/2]$; equation (10) describes the top-left portion of the Arctic Circle, which is the limit shape of 2-enumerated ASMs.

4. Limit shapes of 1- and 3-enumerated ASMs

We start with considering the case of 1-enumerated ASMs. In this case we have $\Delta = 1/2$ and $t = 1$, and the function $h_N(z; \frac{1}{2}, 1)$ is given by the formula (see, e.g., [25, 26])

$$h_N(z; \frac{1}{2}, 1) = {}_2F_1 \left(\begin{matrix} -N + 1, N \\ 2N \end{matrix} \middle| 1 - z \right).$$

We write here the hypergeometric function in such a way that the third parameter is positive, and larger than the second one, so that the Euler integral representation for Gauss hypergeometric function can be used to study the large N limit.

Explicitly, the Euler integral representation gives the following expression

$$h_N(z; \frac{1}{2}, 1) = \frac{\Gamma(2N)}{[\Gamma(N)]^2} \int_0^1 [\tau(1 - \tau)(1 - \tau + z\tau)]^{N-1} d\tau. \quad (11)$$

The large N behaviour of this integral can be found via the standard saddle-point analysis, which in fact can provide a uniform asymptotic expression in z . Hence in evaluating the last term in (9) we can use the property that the logarithmic derivative and the large N limit commute (this property can also be verified directly for integral representation (11)). Explicitly, we find that, as $N \rightarrow \infty$,

$$\log h_N(z; \frac{1}{2}, 1) = N \log [4v(1 - v)(1 - v + zv)] + o(N),$$

where

$$v := \frac{2 - z - \sqrt{z^2 - z + 1}}{3(1 - z)}.$$

Upon differentiating with respect to z , we obtain that the reduced saddle-point equation in this case reads

$$\frac{y}{z - 1} - \frac{1 - x + y}{z} + \frac{1 - \sqrt{z^2 - z + 1}}{z(1 - z)} = 0. \quad (12)$$

The requirement that equation (12) has two coinciding roots gives the following parametric solution for the limit shape of large ASMs:

$$x = 1 - \frac{2\omega - 1}{2\sqrt{\omega^2 - \omega + 1}}, \quad y = 1 - \frac{\omega + 1}{2\sqrt{\omega^2 - \omega + 1}}, \quad \omega \in [1, \infty).$$

Eliminating ω from this parametric solution we obtain that the limit shape is described by the equation

$$4x(1 - x) + 4y(1 - y) + 4xy = 1, \quad x, y \in [0, \frac{1}{2}]. \quad (13)$$

Formula (13) is the central result of our paper. A comparison of this formula with available numerical data is discussed below.

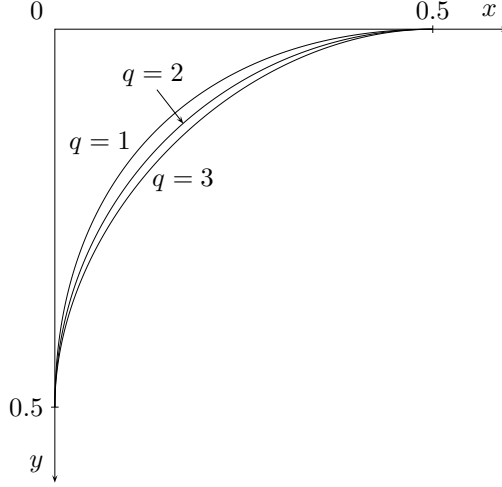


FIGURE 3. The limit shapes of q -enumerated ASMs for $q = 1, 2, 3$, given by equations (13), (10), and (16), respectively.

Let us now consider the case of 3-enumerated ASMs ($\Delta = -1/2$ and $t = 1$). The function $h_N(z; -\frac{1}{2}; 1)$ has been obtained in [25] (see also [26]). The following formulae are valid

$$h_N(z; -\frac{1}{2}; 1) = \begin{cases} (1/2)(z+1)B_{2m}(z) & \text{for } N = 2m + 2, \\ (1/9)(2z+1)(z+2)B_{2m}(z) & \text{for } N = 2m + 3, \end{cases}$$

where $B_{2m}(z)$ is the following polynomial of degree $2m$:

$$B_{2m}(z) = \frac{m+1}{3^{m-1}(2m+3)} z^m (z+2)^m {}_2F_1 \left(\begin{matrix} -m, m+2 \\ 2m+4 \end{matrix} \middle| \frac{z^2-1}{z(z+2)} \right) - \frac{m}{3^{m-1}(2m+3)} z^m (z+2)^{m-1} {}_2F_1 \left(\begin{matrix} -m+1, m+2 \\ 2m+4 \end{matrix} \middle| \frac{z^2-1}{z(z+2)} \right).$$

Again, in comparison with [26], we have written here the hypergeometric polynomials in such a way that the Euler integral formula can be directly applied.

Evaluating the integrals through the saddle-point method, we obtain that, as $N \rightarrow \infty$,

$$\log h_N(z; -\frac{1}{2}, 1) = N \log \left[\frac{2(2z+1)(z+2)}{9(z+1)} \right] + o(N).$$

The reduced saddle-point equation reads:

$$\frac{y}{z-1} - \frac{1-x}{z} - \frac{y}{2+z} + \frac{2z^2+4z+3}{(1+z)(2+z)(1+2z)} = 0. \quad (14)$$

The requirement that equation (14) has two coinciding roots gives us the following parametric solution for the limit shape of 3-enumerated ASMs:

$$x = \frac{7\omega^4 + 14\omega^3 + 19\omega^2 + 12\omega + 2}{(\omega^2 + 2)(2\omega + 1)^2(\omega + 1)^2},$$

$$y = \frac{(\omega - 1)^2(6\omega^4 + 16\omega^3 + 19\omega^2 + 16\omega + 6)}{3(\omega^2 + 2)(2\omega + 1)^2(\omega + 1)^2}, \quad \omega \in [1, \infty). \quad (15)$$

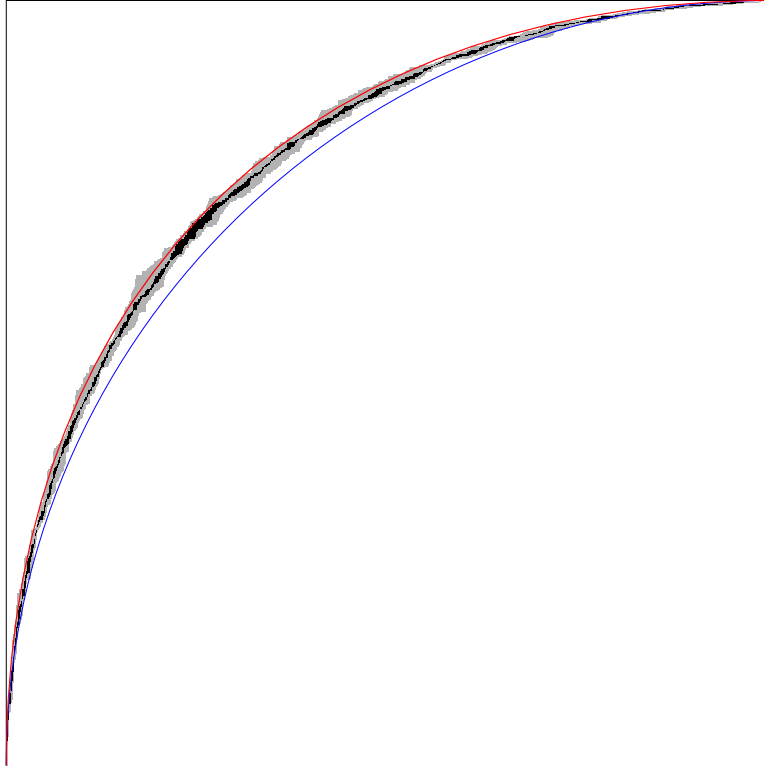


FIGURE 4. Comparison of equation (13) for the limit shape of large ASMs, the outer curve (in red), with the numerical data of [14] for $N = 1500$. The inner curve (in blue) is the Arctic circle, equation (10), plotted here for reference.

Equivalently, one can search for the equation connecting x and y . In this way we obtain that the limit shape of 3-enumerated ASMs is described by the following sextic equation:

$$\begin{aligned}
& 324x^6 + 1620x^5y + 3429x^4y^2 + 4254x^3y^3 + 3429x^2y^4 + 1620xy^5 + 324y^6 \\
& - 972x^5 - 1458x^4y - 2970x^3y^2 - 2970x^2y^3 - 1458xy^4 - 972y^5 \\
& - 6147x^4 - 9150x^3y - 17462x^2y^2 - 9150xy^3 - 6147y^4 \\
& + 13914x^3 + 24086x^2y + 24086xy^2 + 13914y^3 \\
& - 11511x^2 - 17258xy - 11511y^2 \\
& + 4392x + 4392y - 648 = 0, \quad x, y \in [0, \frac{1}{2}]. \quad (16)
\end{aligned}$$

One can verify directly that this equation is indeed satisfied by x and y given by (15).

Figure 3 shows plots of the limit shapes for 1-, 2- and 3-enumerated ASMs. The area of the temperate region decreases as q increases, in agreement with both analytical and numerical considerations [19–21].

Concerning expression (13) for the limit shape of large ASMs, it is worth mentioning here a comparison of this result with numerical simulations. The most refined numerical simulations of large ASMs (up to $N = 1500$) presently available have been performed by Wieland [14], who also provided pictures comparing these numerical data with equation (13)¹. As the size of ASMs increases, convergence to this curve is observed. Although the convergence is rather slow, and more refined data would be welcome, a good agreement is already obtained.

In figure 4 we have elaborated the data of [14] for ten random samples of ASMs of size $N = 1500$, generated using Propp-Wilson ‘coupling from the past’ algorithm (see [14] for further details). Each pixel of the picture corresponds to one of the entries of (the top-left quarter of) the matrix, and has been assigned to one of five bins, according to the frequency of being, in the ten random samples of ASMs, in the frozen region. The five bins are defined by the breakpoints of 5%, 35%, 65%, and 95%. The picture plots the three central bins in grey, black, and grey again, respectively. The picture plots also the analytic expression (13) for the limit shape of large ASMs (the outer curve, in red), and, for reference, equation (10) for the Arctic Circle (the inner curve, in blue).

Acknowledgements

We thank B. Wieland for providing us his data on heavy simulations for the limit shape of ASMs and making useful pictures of them. This work is partially done within the European Science Foundation program INSTANS. One of us (AGP) is supported in part by Russian Foundation for Basic Research (grant 07-01-00358), and by the programme “Mathematical Methods in Nonlinear Dynamics” of Russian Academy of Sciences. AGP also thanks INFN, Sezione di Firenze, where part of this work was done, for hospitality and support. Finally, we would like to thank two anonymous referees for their constructive comments which stimulated us to improve the presentation of the paper.

References

- [1] D. M. Bressoud, *Proofs and confirmations: The story of the alternating sign matrix conjecture*, Cambridge University Press, Cambridge, 1999.
- [2] J. Propp, *The many faces of alternating-sign matrices*, Discrete Models: Combinatorics, Computation, and Geometry, DM-CCG 2001, DMTCS Proceedings, vol. AA, Discrete Mathematics and Theoretical Computer Science, 2001, 43–58 pp., arXiv:math/0208125.
- [3] W. Jockush, J. Propp, and P. Shor, *Random domino tilings and the arctic circle theorem*, arXiv:math.CO/9801068.
- [4] H. Cohn, M. Larsen, and J. Propp, *The shape of a typical boxed plane partition*, New York J. Math. **4** (1998), 137–165, arXiv:math/9801059.
- [5] N. Elkies, G. Kuperberg, M. Larsen, and J. Propp, *Alternating-sign matrices and domino tilings*, J. Algebraic Combin. **1** (1992), 111–132, 219–234.
- [6] G. Kuperberg, *Another proof of the alternative-sign matrix conjecture*, Int. Math. Res. Not. **1996** (1996), 139–150, arXiv:math/9712207.
- [7] D. Zeilberger, *Proof of the refined alternating sign matrix conjecture*, New York J. Math. **2** (1996), 59–68, arXiv:math/9606224.
- [8] V. E. Korepin, *Calculations of norms of Bethe wave functions*, Commun. Math. Phys. **86** (1982), 391–418.
- [9] A. G. Izergin, *Partition function of the six-vertex model in the finite volume*, Sov. Phys. Dokl. **32** (1987), 878–879.

¹Pictures and the C program code are available upon request.

- [10] A. G. Izergin, D. A. Coker, and V. E. Korepin, *Determinant formula for the six-vertex model*, J. Phys. A **25** (1992), 4315–4334.
- [11] R. J. Baxter, *Exactly solved models in statistical mechanics*, Academic Press, San Diego, CA, 1982.
- [12] F. Colomo and A. G. Pronko, *Emptiness formation probability in the domain-wall six-vertex model*, Nucl. Phys. B **798** (2008), 340–362, arXiv:0712.1524.
- [13] F. Colomo and A. G. Pronko, *The Arctic Circle revisited*, Contemp. Math. **458** (2008), 361–376, arXiv:0704.0362.
- [14] B. Wieland, Message of Jan 10, 2008, on Domino Forum and private communication.
- [15] N. M. Bogoliubov, A. G. Pronko, and M. B. Zvonarev, *Boundary correlation functions of the six-vertex model*, J. Phys. A **35** (2002), 5525–5541, arXiv:math-ph/0203025.
- [16] L. A. Takhtadjan and L. D. Faddeev, *The quantum method of the inverse problem and the Heisenberg XYZ model*, Russian Math. Surveys **34** (1979), no. 5, 11–68.
- [17] V. E. Korepin, N. M. Bogoliubov, and A. G. Izergin, *Quantum inverse scattering method and correlation functions*, Cambridge University Press, Cambridge, 1993.
- [18] N. Kitanine, J.-M. Maillet, N. A. Slavnov, and V. Terras, *Spin-spin correlation functions of the XXZ-1/2 Heisenberg chain in a magnetic field*, Nucl. Phys. B **641** (2002), 487–518, arXiv:hep-th/0201045.
- [19] V. E. Korepin and P. Zinn-Justin, *Thermodynamic limit of the six-vertex model with domain wall boundary conditions*, J. Phys. A **33** (2000), 7053–7066, arXiv:cond-mat/0004250.
- [20] O. F. Syljuåsen and M. B. Zvonarev, *Monte-Carlo simulations of vertex models*, Phys. Rev. E **70** (2004), 016118, arXiv:cond-mat/0401491.
- [21] D. Allison and N. Reshetikhin, *Numerical study of the 6-vertex model with domain wall boundary conditions*, Ann. Inst. Fourier (Grenoble) **55** (2005), 1847–1869, arXiv:cond-mat/0502314.
- [22] L. Paniak and N. Weiss, *Kazakov-Migdal model with logarithmic potential and the double Penner matrix model*, J. Math. Phys. **36** (1995), 2512–2530, arXiv:hep-th/9501037.
- [23] J. Ambjorn, Yu. Makeenko, and C. F. Kristjansen, *Generalized Penner models to all genera*, Phys. Rev. D **50** (1994), 5193–5203, arXiv:hep-th/9403024.
- [24] R. C. Penner, *Perturbative series and the moduli space of Riemann surfaces*, J. Diff. Geom. **28** (1988), 35–53.
- [25] F. Colomo and A. G. Pronko, *On the refined 3-enumeration of alternating sign matrices*, Adv. in Appl. Math. **34** (2005), 798–811, arXiv:math-ph/0404045.
- [26] F. Colomo and A. G. Pronko, *Square ice, alternating sign matrices, and classical orthogonal polynomials*, J. Stat. Mech. Theory Exp. (2005), P01005, arXiv:math-ph/0411076.

INFN, SEZIONE DI FIRENZE, VIA G. SANSONE 1, 50019 SESTO FIORENTINO (FI), ITALY
E-mail address: colomo@fi.infn.it

SAINT PETERSBURG DEPARTMENT OF V.A. STEKLOV MATHEMATICAL INSTITUTE OF RUSSIAN
 ACADEMY OF SCIENCES, FONTANKA 27, 191023 SAINT PETERSBURG, RUSSIA
E-mail address: agp@pdmi.ras.ru